

Pump-Probe Spectroscopy of Two-Body Correlations in Ultracold Gases

Christiane P. Koch^{1,*} and Ronnie Kosloff²

¹*Institut für Theoretische Physik, Freie Universität Berlin, Arnimallee 14, 14195 Berlin, Germany*

²*Institute of Chemistry and The Fritz Haber Research Center, The Hebrew University, Jerusalem 91904, Israel*

(Received 20 May 2009; published 21 December 2009)

We suggest pump-probe spectroscopy to study pair correlations that determine the many-body dynamics in weakly interacting, dilute ultracold gases. A suitably chosen, short laser pulse depletes the pair density locally, creating a “hole” in the electronic ground state. The dynamics of this nonstationary pair density is monitored by a time-delayed probe pulse. The resulting transient signal allows us to spectrally decompose the hole and to map out the pair correlation function.

DOI: 10.1103/PhysRevLett.103.260401

PACS numbers: 03.75.Kk, 32.80.Qk, 82.53.Kp

Introduction.—Bose-Einstein condensation in dilute gases is determined by the nature of the two-body interactions between the atoms [1]. These microscopic interactions manifest themselves in two-body correlations and dictate the mesoscopic and macroscopic properties of the condensate. Formally, the dynamics of an ultracold gas is described in terms of field equations [1]. For dilute gases where only two-body interactions are prominent, the equation of motion for the field operator that annihilates (or creates) a particle at position \vec{x} reads

$$i\hbar \frac{\partial \hat{\psi}}{\partial t}(\vec{x}; t) = \hat{H}_1 \hat{\psi}(\vec{x}; t) + \int d^3\vec{y} \hat{V}_2(\vec{x} - \vec{y}) \hat{\psi}^\dagger(\vec{y}; t) \hat{\psi}(\vec{y}; t) \hat{\psi}(\vec{x}; t). \quad (1)$$

Expectation values of the many-body system can be expressed in terms of normal-ordered correlation functions. To lowest order, these are the condensate or mean field wave function, $\Psi(\vec{x}; t) = \langle \hat{\psi}(\vec{x}; t) \rangle$, the one-body density matrix $R(\vec{x}, \vec{y}; t) = \langle \hat{\psi}^\dagger(\vec{x}; t) \hat{\psi}(\vec{y}; t) \rangle$ and the pair correlation function, $\Phi(\vec{x}, \vec{y}; t) = \langle \hat{\psi}(\vec{x}; t) \hat{\psi}(\vec{y}; t) \rangle$. For practical calculations, the infinite set of equations of motion for the many-body problem needs to be truncated. This can be achieved by expanding the correlation functions into cumulants [2]. A separation of time or length scales, i.e., small collision time vs long free propagation time or small effective range of the interaction potential vs large interatomic distance is required to justify truncation. For dilute Bose gases in a macroscopic trap, such an assumption can typically be made, and within the first-order cumulant expansion, the dynamics of pair correlations is decoupled from higher order terms [2]. Alternatively, one can work with the correlation functions directly [3]. In both cases, the dynamics of the macroscopic pair correlation function is described by a Schrödinger-like equation where the mean field enters as a source term [2] or acts as an additional potential [3]. If we restrict our considerations to time scales that are much shorter than the time scale of the mean

field dynamics, the pair correlation dynamics are described by a standard Schrödinger equation where the presence of the condensate only modifies the boundary conditions. The macroscopic pair correlation function is then given by the two-body wave function of an isolated pair of atoms, $\Phi(r)$ with $r = |\vec{x} - \vec{y}|$. We can thus study the many-body pair correlation dynamics by solving the time-dependent Schrödinger equation for two colliding atoms [3].

In the most simplified approach, the effect of the many-body pair correlations is captured in a single parameter, the scattering length [1]. Measuring the scattering length corresponds to an indirect assessment of the pair correlations. If the two-body interaction is probed in a time much shorter than its characteristic time scale, a more comprehensive study becomes possible. Here we suggest to employ pump-probe spectroscopy to unravel the dynamics of pair correlations in an ultracold Bose gas. This requires a

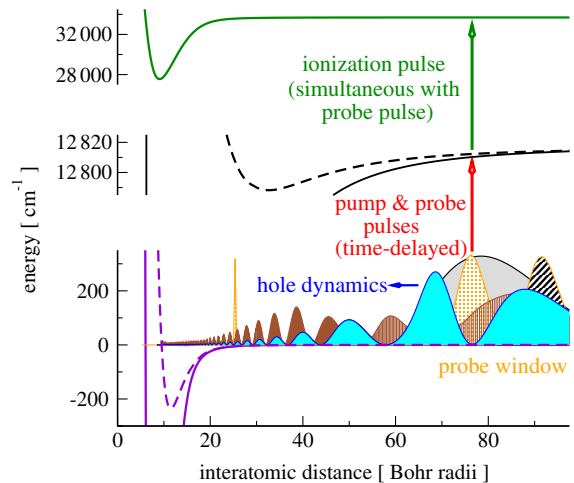


FIG. 1 (color online). Pump-probe spectroscopy of dynamical pair correlations: A pump pulse excites population from the electronic ground state, leaving the pair correlation function in a nonstationary state, the hole. A time-delayed probe pulse monitors the dynamics of the hole. The orange peaks indicate the region where the probe pulse measures pair amplitude.

combination of ultrafast and ultracold physics, the basic feasibility of which has been demonstrated in recent experiments on femtosecond photoassociation of ultracold rubidium atoms [4,5].

Pump-probe spectroscopy.—Our scheme involves three short laser pulses and is sketched in Fig. 1 for the example of an ultracold gas of ^{87}Rb atoms. The pump pulse excites population from the electronic ground to an excited state, leaving a hole in the initial pair correlation function. The hole represents a nonstationary state that moves under the influence of the ground state potential; cf. Fig. 1. The pump pulse thus induces the dynamics of the pair correlations. A time-delayed probe monitors these dynamics by measuring the amount of probability amplitude in a range of internuclear distances. The measurement consists of applying simultaneously a photoassociation and an ionization pulse (combination of red and green arrows in Fig. 1). The pair density on the ground state is thus photoassociated and immediately ionized for detection. The largest probe signal is obtained when the probe pulse is identical to the pump pulse. The dynamics are then monitored at the position where the hole was created. The spatial region where the probe pulse detects pair density is indicated in orange in Fig. 1.

For alkali atoms, the initial pair correlation function consists of a superposition of singlet and triplet components. The corresponding interaction potentials are shown in solid (singlet) and dashed (triplet) lines. For clarity's sake, only triplet pair wave functions are depicted in Fig. 1. Since the respective excited state potentials differ, the probe pulse is resonant at different interatomic distances for singlet and triplet. This is indicated by the orange peaks representing the probe windows in Fig. 1 (striped for singlet, dotted for triplet).

Detection of the pair correlation dynamics proceeds via the creation of molecular ions and is inspired by Refs. [4,5]. In those experiments, the pump pulse photoassociates ultracold atoms and the ensuing excited state molecular dynamics are detected by the ionization pulse. In contrast to that, it is the ground state dynamics of the many-body pair correlations that are probed in our proposal; photoassociation just serves as a means for detection. Hence, while the experimental setups envisioned in this work and realized in Refs. [4,5] are similar, the probed physics is rather different.

Modelling the two-body interaction.—We consider two colliding ^{87}Rb atoms. Hyperfine interaction couples the ground state singlet and lowest triplet scattering channels. However, this interaction cannot be resolved on the time scales considered below. We therefore assume a superposition of singlet and triplet components, but neglect the effect of hyperfine interaction on binding energies and dynamics. The two-body Hamiltonian is represented on a grid large enough to faithfully represent the scattering atoms. The interaction of the atom pair with the pump pulse is treated within the dipole and rotating wave approximations. Excitation is considered exemplarily into the

$0_u^+(5s + 5p_{3/2})$ and $0_g^-(5s + 5p_{3/2})$ excited states. The pulses are taken to be transform-limited Gaussian pulses with a full-width at half-maximum (FWHM) of 10 ps. This corresponds to a spectral bandwidth of roughly 1.5 cm^{-1} or 45 GHz. Details on the potentials and the employed methods are found in Ref. [6]. For a Bose-Einstein condensate, a single low energy scattering state needs to be considered. The collision energy of this initial state is chosen to correspond to 20 μK with 75% (25%) triplet (singlet) character. At higher temperatures, the bosonic nature of the atoms can be neglected, and the ultracold thermal ensemble is described by a Boltzmann average over all thermally populated two-body scattering states [7].

Modeling the absorption of the probe pulse.—The dynamics of the nonstationary hole is monitored by a combination of a probe pulse and an ionization pulse; cf. Fig. 1. This two-color scheme converts the absorption of the probe pulse into detection of molecular ions. Assuming the probe pulse to be weak and the ionization step to be saturated, absorption of the probe pulse can be modeled within first-order perturbation theory [8,9]. The transient absorption signal is then represented by the time-dependent expectation value of a window operator,

$$\hat{W}(\hat{r}) = \pi(\tau_p E_{p,0})^2 e^{-2\hat{\Delta}(\hat{r})^2 \tau_p^2} \cdot \hat{\boldsymbol{\mu}}^2, \quad (2)$$

where τ_p and $E_{p,0}$ denote duration (FWHM) and peak amplitude of the probe pulse. $\hat{\boldsymbol{\mu}}$ is the transition dipole moment between ground and first excited state. The central frequency of the probe pulse, ω_p , determines the difference potential, $\hat{\Delta}(\hat{r}) = V_e(\hat{r}) - V_g(\hat{r}) - \hbar\omega_p$. A position measurement becomes possible if the difference between the ground and excited state potential is sufficiently large, and, moreover, the spectral bandwidth sufficiently small to probe only nonzero $\hat{\Delta}(\hat{r})$. Since the difference potential vanishes for $r \rightarrow \infty$, this implies sufficiently detuned, narrow-band probe pulses. Figure 1 shows triplet and singlet window operators (orange peaks) assuming identical parameters for pump and probe pulses.

Characterization of the hole.—As sketched in Fig. 1, the pump pulse carves a 'hole' into the ground state pair correlation function. The resulting nonstationary wave packet is a superposition of a few weakly bound vibrational wave functions and many scattering states [10]. The detuning of the pump pulse from the atomic resonance frequency, $\Delta_L = \omega_L - \omega_{\text{at}}$, determines the position where the hole is created: For larger detuning, excitation occurs at shorter distance and populates deeper bound levels. A pulse energy of $\mathcal{E}_p = 1.5 \text{ nJ}$ is sufficient to deplete the population within the resonance window of the pump pulse (cf. the blue wave function in Fig. 1). At higher pulse energies, Rabi cycling within the resonance window sets in. This leads to more population in the bound levels but also to stronger redistribution among the scattering states.

Dynamics of the hole.—Figure 1 also illustrates the time evolution of the pair correlation amplitude after a weak pump pulse ($\mathcal{E}_p = 1.5 \text{ nJ}$) has been applied: The blue

curve depicts the wave function just after the pump pulse, at $t = 24$ ps (taking $t = 0$ to be the time of the pump pulse maximum). A probe measurement at that time will find no amplitude within the probe window. Because of the attractive interaction potential, the hole moves toward shorter distances; cf. the brown wave function ($t = 126$ ps). This brings amplitude that is initially at larger r into the probe window. Eventually the motion of the hole will be reflected at the repulsive barrier of the potential. The bound part of the wave packet will remain at short distance and oscillate, while the scattering part will pass through the probe window once not to return.

Pump-probe spectra.—The dynamics of the hole is reflected in the transient probe absorption, i.e., the time-dependent expectation value of the window operator [red dotted curve in Fig. 2(a)]: A depletion of the signal due to the creation of the hole by the pump pulse, referred to as “bleach” in traditional pump-probe spectroscopy, is followed by a recovery that peaks at 550 ps. At later times oscillations due to partial recurrence are observed but a full recovery does not occur. Rabi cycling induced by larger pulse energies may partially (green solid curve) or completely (blue dashed curve) refill the hole. For larger detuning, cf. Fig. 2(b), the hole is created at shorter interatomic distance, $r \sim 48a_0$ for $\Delta_L = -14$ cm $^{-1}$ vs $r \sim 76a_0$ for $\Delta_L = -4$ cm $^{-1}$. Obviously, the time to move to the repulsive barrier and back is then shorter. A faster recovery of the bleach is hence observed—at $t = 110$ ps in Fig. 2(b).

The spectrum of the transient absorption signals shown in Fig. 2 can be obtained by filter-diagonalization [11], a method allowing to accurately extract frequencies from just a few oscillation periods. The spectra are shown in Fig. 3. The vibrational energies of the two-body interaction potential are recovered. Figure 3 shows furthermore that

Rabi cycling during the pump pulse leads to a larger bound part in the hole; cf. the increase of spectral weights with pump pulse energy. While a direct measurement of the vibrational populations would be difficult to implement experimentally, wave packet spectral analysis via probe absorption is fairly straightforward.

Pure state vs thermally averaged dynamics.—Pump-probe spectroscopy of the pair correlations can be applied to a condensate as well as a thermal ultracold gas. For the time scales considered here, this translates into comparing the dynamics of a pure state to that of an incoherent ensemble. Figure 4 shows the transient probe absorption for the two cases. Thermal averaging markedly smears out the recovery of the bleach at 550 ps. In principle, thermal averaging introduces two effects—the finite width in scattering energies which is too small to be resolved on a nanosecond time scale, and the contribution of higher partial waves. The latter becomes particularly prominent in the presence of resonances. Figure 4 compares calculations including both singlet and triplet channels (a) to those for the triplet component only (b) in order to highlight the role of shape resonances. For ^{87}Rb , shape resonances are found at ~ 160 μK ($J = 2$) and at ~ 430 μK ($J = 6$) in the singlet, and for $J = 2$ at ~ 290 μK in the triplet channel. The second peak observed in Fig. 4(a) at 1100 ps corresponds to the singlet recovery of the bleach. The shape resonances lead to a much larger weight of the singlet contribution in the thermal averages than in the pure state s -wave calculation. Since probe absorption in the singlet channel occurs at larger distances than for the triplet channel, cf. Fig. 1, the recovery of the bleach is observed at later times. This observation opens up the perspective of analyzing pair correlation functions in coupled channels scattering near a resonance where tuning an external field

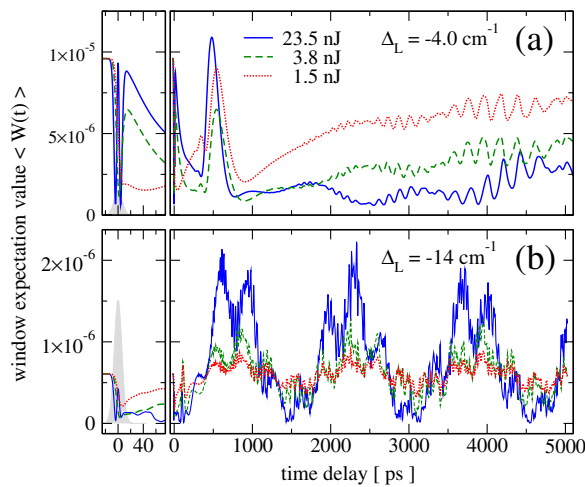


FIG. 2 (color online). Probing the two-body correlation dynamics: Absorption of the probe pulse as a function of the delay between pump and probe pulses. The pump pulse detunings are $\Delta_L = -4.0$ cm $^{-1}$ (a) and $\Delta_L = -14$ cm $^{-1}$ (b), and three different pump pulse energies are shown.

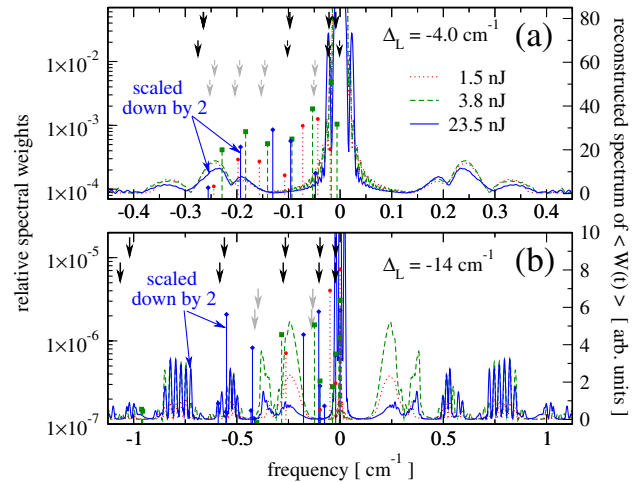


FIG. 3 (color online). Spectra of the transient absorption signals shown in Fig. 2. The eigenenergies of the interaction potential are recovered: Black arrows indicate the position of the binding energies of the triplet (upper row) and singlet (lower row) levels, grey arrows half-multiples of the binding energies. The spectra for 23.5 nJ (blue solid lines) are scaled down by a factor of 2.

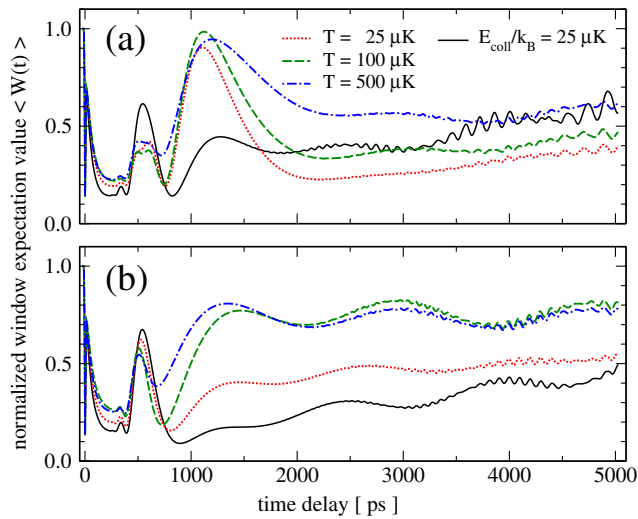


FIG. 4 (color online). Absorption of the probe pulse as a function of the delay between pump and probe pulses comparing pure state dynamics (black solid lines) to those of a thermal ensemble (colored broken lines). (a) Calculation including two scattering channels (singlet and triplet): The thermal dynamics are dominated by a singlet shape resonance while the pure dynamics shows features of both singlet and triplet dynamics. (b) Calculation for a single channel (triplet): The thermal and pure state dynamics are similar with the recovery of the bleach smeared out at higher temperatures. ($\Delta_L = -4.0 \text{ cm}^{-1}$, $\mathcal{E}_p = 3.8 \text{ nJ}$).

through the resonance will modify the respective weight of the channels. We emphasize that this novel pair correlation spectroscopy is possible even in the presence of, e.g., three-body losses as long as the decay occurs on a time scale larger than a few nanoseconds.

Mapping out the pair correlation function.—Pump-probe spectroscopy, a well established tool in chemical physics, allows for retrieving the amplitude and phase of a wave function [12]. In the present context we can retrieve the pair correlation density operator $\rho(r, r', t)$ with $\rho(r, r'; t) = \Phi(r; t)\Phi^*(r'; t)$ for a BEC. This is based on Eq. (2), where probe absorption corresponds to a position measurement with finite resolution: Different central frequencies, ω_p , define the position that is measured, and the difference potential, $\hat{\Delta}(\hat{r})$, together with the pulse duration, τ_p , controls the resolution. These measurements resolve the amplitude of the pair correlation, $|\Phi^*(r'; t)|^2$. The phase information is obtained by chirping the probe pulse which corresponds to a momentum measurement [9]. The window operator then defines a finite resolution measurement in phase space [13]. Collecting the expectation values for a sufficiently large set of window operators with different positions (frequencies) and momenta (chirps) corresponds to quantum state tomography of $\rho(r, r'; t)$ [14].

Conclusions.—Pump-probe spectroscopy unravels directly many-body pair correlations in dilute Bose gas.

Existing experimental setups [4,5] need to be only slightly modified to implement our proposal. In particular, transform-limited pulses of about 1 cm^{-1} bandwidth are required for detection of the probe absorption via molecular ions. Spectral features on a scale of less than 1 cm^{-1} can be resolved for pump-probe delays of a few nanoseconds. Pump-probe spectroscopy of the pair correlations dynamics allows us to capture transient states of ultracold gases such as collapsing condensates. Moreover, it can be combined with static external field control. For example, tuning a magnetic field close to a Feshbach resonance may enhance the pair density at short and intermediate distances [15]. The resulting coupled channels pair correlation function can be mapped out despite the finite lifetime of the resonance. Future work will consider shaped pulses. Once picosecond pulse shaping becomes available, the full power of coherent control can be employed to study pair correlation dynamics.

We are grateful to F. Masnou-Seeuws and P. Naidon for many fruitful discussions, to our referees for helpful comments and to the Deutsche Forschungsgemeinschaft for financial support.

*ckoch@physik.fu-berlin.de

- [1] C. J. Pethick and H. Smith, *Bose-Einstein Condensation in Dilute Gases* (Cambridge University Press, Cambridge, England, 2002); A. J. Leggett, *Rev. Mod. Phys.* **73**, 307 (2001).
- [2] T. Köhler and K. Burnett, *Phys. Rev. A* **65**, 033601 (2002); T. Köhler, T. Gasenzer, and K. Burnett, *Phys. Rev. A* **67**, 013601 (2003).
- [3] P. Naidon and F. Masnou-Seeuws, *Phys. Rev. A* **68**, 033612 (2003); P. Naidon and F. Masnou-Seeuws, *Phys. Rev. A* **73**, 043611 (2006).
- [4] W. Salzmann *et al.*, *Phys. Rev. Lett.* **100**, 233003 (2008).
- [5] D. J. McCabe *et al.*, *Phys. Rev. A* **80**, 033404 (2009).
- [6] C. P. Koch, R. Kosloff, and F. Masnou-Seeuws, *Phys. Rev. A* **73**, 043409 (2006); C. P. Koch, F. Masnou-Seeuws, and R. Kosloff, *Phys. Rev. Lett.* **94**, 193001 (2005).
- [7] C. P. Koch *et al.*, *J. Phys. B* **39**, S1017 (2006).
- [8] L. W. Ungar and J. A. Cina, *Adv. Chem. Phys.* **100**, 171 (1997).
- [9] E. Gershgoren *et al.*, *J. Phys. Chem. A* **105**, 5081 (2001).
- [10] E. Luc-Koenig, F. Masnou-Seeuws, and R. Kosloff, *Phys. Rev. A* **76**, 053415 (2007).
- [11] V. A. Mandelshtam and H. S. Taylor, *J. Chem. Phys.* **107**, 6756 (1997); V. A. Mandelshtam and H. S. Taylor, *J. Chem. Phys.* **108**, 9970 (1998).
- [12] K. Ohmori *et al.*, *Phys. Rev. Lett.* **96**, 093002 (2006).
- [13] C. P. Koch and R. Kosloff (to be published).
- [14] *Quantum State Estimation*, edited by M. Paris and J. Řeháček, *Lecture Notes in Physics Vol. 649* (Springer, Berlin Heidelberg, 2004).
- [15] P. Pellegrini, M. Gacesa, and R. Côté, *Phys. Rev. Lett.* **101**, 053201 (2008).